J. Fluid Mech. (1966), *vol.* 25, *part* 1, *pp.* 17–41
Printed in Great Britain

The method of characteristics for the three-dimensional unsteady magnetofluid dynamics of a multi-component medium

By HARRY SAUERWEIN

Fluid Physics Department, Aerospace Corporation,
San Bernardino, California

(Received 12 March 1965 and in revised form 11 August 1965)

A general numerical method of characteristics applicable to problems in magnetofluid dynamics as well as ordinary fluid dynamics is described. The method can be applied to unsteady three-dimensional flows of chemically reacting, non-equilibrium, multi-component media. Dissipative phenomena must be neglected in order to make the governing equations of change hyperbolic, because the method can be applied only to quasi-linear, hyperbolic, partial differential equations. Practical restrictions on computation time usually require unsteady problems to be limited to cases with short transient times although theoretically the method applies to all unsteady flows. In steady flow the local velocity must be greater than the largest local wave speed. The characteristic and compatibility equations are derived for the most general case of magnetofluid dynamics. A new finite-difference network and its corresponding equations are developed similarly. Specialization of the general method to consider simpler problems is outlined. Preliminary numerical results of calculations using the method are presented. The practicality and feasibility of utilizing the general numerical method of characteristics on presently available, electronic digital computers is evaluated in the light of recent experience in calculating multi-dimensional flows with the method.

1. Introduction

This paper discusses a finite-difference technique applicable to the quasi-linear hyperbolic partial differential equations obtained from the equations of fluid dynamics by neglecting all terms which arise from dissipative processes. The numerical method of characteristics discussed here refers to a method which uses the properties of characteristic directions to simplify the partial differential equations before putting them in finite-difference form. The finite-difference calculation proceeds along characteristic surfaces so that domains of dependence are explicitly determined, and numerical stability and convergence criteria are more easily obtained and fulfilled. The numerical method of characteristics has been used extensively for flow problems involving two independent variables; see, for example, Meyer (1953) and Ferri (1954). The method applied to three independent variables has been considered by Thornhill (1948), Coburn & Dolph (1949), Sauer (1950), Holt (1956), and Fowell (1961), but only recently

have actual numerical calculations been attempted by Butler (1960), Tsung (1960), and Moretti *et al.* (1962). The method can be extended to problems involving four independent variables, three space co-ordinates and time, as was done by Bruhn & Haack (1958), Sauerwein (1964) and Strom (1965), but actual numerical calculations have not as yet been accomplished principally because of the limitations of existing computers. The next generation of computers should be capable of handling at least the simpler four-variable problems.

This paper presents with a unified approach the method as applied to three-dimensional, unsteady, ordinary fluid dynamics. The method is then extended to magnetofluid dynamics. A new finite-difference scheme, developed from the results of recent numerical calculations, is presented. This scheme has several advantages in its application to the general method, which are detailed below.

The method of characteristics uses the fundamental property of characteristic surfaces that, when the equations are written in characteristic form, derivatives in a direction normal to the characteristic surfaces do not appear in the equations. In two-variable problems, a simplification is brought about by using characteristic directions because the partial differential equations are reduced to ordinary differential equations, which can be integrated along characteristic lines. In problems of more than two variables, however, this simplification does not result because the equations in characteristic form are still partial differential equations. The reduction in the number of partial derivatives which appear explicitly in the equations is still a simplification which can be successfully utilized. The equations can still be integrated in certain characteristic directions with the partial derivatives in the other directions evaluated numerically by finite-difference techniques. In addition to reducing the number of partial derivatives, the method of characteristics determines the solution on characteristic surfaces which bound the domains of dependence and regions of influence of points. Explicit knowledge of the location of the surfaces can be used to understand the physical propagation of waves in the flow (because the characteristic surfaces are the envelopes of waves in the flow field), and can be used to simplify stability and convergence determination for the finite-difference procedure.

The calculation of certain unsteady flows is restricted because of a practical limitation on the numerical calculation. This limitation does not apply to steady flow problems, but the equations must be hyperbolic for the method to apply there. This generally means that the steady flow must be 'supersonic' in some sense; i.e. the local flow velocity must be greater than the local wave speed of the fastest wave possible in the medium. The practical limitation on unsteady flow can be seen by referring to figure 1. Consider a one-dimensional, unsteady situation which shows the basic limitation even for the multi-dimensional case. Consider a fluid particle at the origin at $t = 0$ which moves in a steady flow with velocity u and is located at P after a time Δt. The wave speed in the medium is c. Only points between A and B at $t = 0$ can influence P. Taking this as a basic, finite-difference network, with the flow to be determined at P from conditions at A and B, it can be seen that

$$\Delta t = \Delta x/2c. \tag{1.1}$$

If $\Delta x = 1$ ft. and the medium is air ($c \approx 1000$ ft./sec), $t \approx 0{\cdot}0005$ sec; thus it can be seen that only very short time steps can be made and, therefore, only problems involving very short transient times can be considered. Hypersonic flows usually have very short transient times so that the method can be applied to hypersonic unsteady flows.

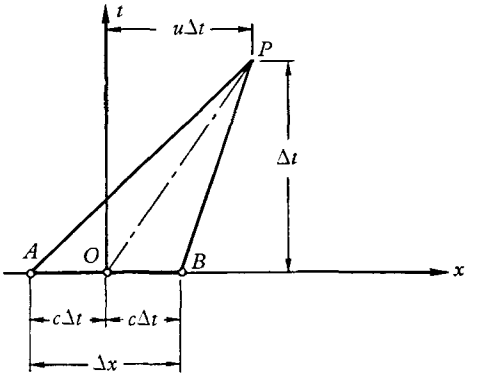

FIGURE 1. Wave geometry.

For multi-dimensional, unsteady problems where the wave speed might vary from place to place in the field and perhaps as a function of its direction of propagation, Δt can be estimated conservatively by

$$\Delta t \approx \Delta x / 2c_{\max}. \tag{1.2}$$

In ordinary fluid dynamics

$$c_{\max} = a_{\max},$$

or in magnetofluid dynamics

$$c_{\max} = \sqrt{(a^2_{\max} + b^2_{\max})},$$

where a is the speed of sound and b is the Alfvén wave speed. Hence, it can be seen that the limitation is just as restricting in multi-dimensional and magnetofluid dynamic flows.

2. The general equations for the method of characteristics

The method of characteristics applies only to hyperbolic, partial differential equations. The equations of magnetofluid dynamics are hyperbolic only if dissipative phenomena are neglected. In many flows of practical interest away from boundaries, where gradients might be large, dissipative effects can be neglected except for electrical resistance. Because of this, the application of the method must be arbitrarily limited to a medium with negligible electrical resistance.

The equations without dissipations are

for over-all continuity

$$\frac{\partial \rho}{\partial t} + \nabla . (\rho \mathbf{V}) = 0, \tag{2.1a}$$

for species continuity

$$\rho \frac{Dc_i}{Dt} = r_i \quad (i = 1, \ldots, N-1), \tag{2.1b}$$

for momentum conservation

$$\rho \frac{D\mathbf{V}}{Dt} + \nabla p - \frac{1}{\mu}(\nabla \times \mathbf{B}) \times \mathbf{B} = 0, \tag{2.1c}$$

for energy conservation

$$\rho \frac{Dh}{Dt} - \frac{Dp}{Dt} = 0, \tag{2.1d}$$

and Maxwell's equations give

$$\frac{\partial \mathbf{B}}{\partial t} - \nabla \times (\mathbf{V} \times \mathbf{B}) = 0, \tag{2.1e}$$

where

$$\frac{D}{Dt} = \frac{\partial}{\partial t} + \mathbf{V} . \nabla,$$

with the thermodynamic relation

$$h = h(p, \rho, c_1, \ldots, c_{N-1}) \tag{2.1f}$$

required to complete the set. ρ, $\mathbf{V}$, c_i, r_i, p, $\mathbf{B}$, h and N are respectively the mass density, the velocity, the mass fraction of the ith species, the chemical source function of the ith species, the pressure, the magnetic induction, the specific enthalpy and the total number of chemical species. Ohm's law has been taken in the standard form, that the current density divided by the electrical conductivity is equal to the electric field plus the vector cross-product of the velocity with the magnetic induction. The usual assumptions of negligible displacement current and net charge density have been made and the MKSQ system of units is employed.

The single algebraic equation (2.1f) can be used to eliminate the enthalpy from (2.1d) to give

$$\frac{D\rho}{Dt} - \frac{1}{a^2}\frac{Dp}{Dt} + \frac{1}{(\partial h/\partial \rho)_{p, c_n}} \sum_{k=1}^{N} \left\{ \frac{Dc_k}{Dt} \left(\frac{\partial h}{\partial c_k} \right)_{p, \rho, c_{n \neq k}} \right\} = 0, \tag{2.2}$$

where the subscripts of the thermodynamic derivatives indicate the properties held constant in the differentiation and

$$c_n = c_1, c_2, \ldots, c_{N-1},$$

$$c_{n \neq k} = c_1, c_2, \ldots, c_{k-1}, c_{k+1}, \ldots, c_{N-1}.$$

'a' is the velocity of sound given by

$$a^2 = -\left(\frac{\partial h}{\partial \rho} \right)_{p, c_n} \Big/ \left\{ \left(\frac{\partial h}{\partial p} \right)_{\rho, c_n} - \frac{1}{\rho} \right\}, \tag{2.3}$$

which is the speed of sound in a gas with the mass fractions of the species held constant, or in other words, the frozen speed of sound as pointed out by Chu (1957) and Broer (1958). Another useful form of the energy equation is obtained by introducing the entropy s into (2.2) to obtain

$$\left(\frac{\partial p}{\partial s} \right)_{\rho, c_n} \frac{Ds}{Dt} = -\sum_{k=1}^{N} \left[\frac{Dc_k}{Dt} \left\{ \left(\frac{\partial p}{\partial c_k} \right)_{s, \rho, c_{n \neq k}} + \frac{(\partial h/\partial c_k)_{p, \rho, c_{n \neq k}}}{(\partial h/\partial p)_{\rho, c_n} - 1/\rho} \right\} \right], \tag{2.4}$$

where we have used $$a^2 = \left(\frac{\partial p}{\partial \rho}\right)_{s,c_n}. \tag{2.5}$$

Equations (2.1), (2.2), and (2.3) are the non-dissipative form of the magneto-fluid dynamic equations to which the numerical method of characteristics can be applied.

Ordinary fluid dynamics

Consider a general case of three-dimensional unsteady flow of a compressible, reacting, multi-component, non-conducting fluid. In Cartesian co-ordinates the equations of change are

$$\frac{D\rho}{Dt} + \rho\left(\frac{\partial u}{\partial x} + \frac{\partial v}{\partial y} + \frac{\partial w}{\partial z}\right) = 0, \tag{2.6a}$$

$$\frac{Du}{Dt} + \frac{1}{\rho}\frac{\partial p}{\partial x} = 0, \tag{2.6b}$$

$$\frac{Dv}{Dt} + \frac{1}{\rho}\frac{\partial p}{\partial y} = 0, \tag{2.6c}$$

$$\frac{Dw}{Dt} + \frac{1}{\rho}\frac{\partial p}{\partial z} = 0, \tag{2.6d}$$

$$\frac{D\rho}{Dt} - \frac{1}{a^2}\frac{Dp}{Dt} + \frac{1}{(\partial h/\partial \rho)_{p,c_n}} \sum_{k=1}^{N} \left\{\frac{Dc_k}{Dt}\left(\frac{\partial h}{\partial c_k}\right)_{p,\rho,c_{n\neq k}}\right\} = 0, \tag{2.6e}$$

$$\frac{Dc_i}{Dt} = \frac{1}{\rho} r_i \quad (i = 1, \ldots, N-1), \tag{2.6f}$$

where u, v, w are the x-, y-, z-components of the velocity vector and

$$\frac{D}{Dt} = \frac{\partial}{\partial t} + u\frac{\partial}{\partial x} + v\frac{\partial}{\partial y} + w\frac{\partial}{\partial z}.$$

Equation (2.4) will be used occasionally instead of (2.6 *e*) and the thermodynamic entropy function, $$s = s(p, \rho, c_1, \ldots, c_{N-1}) \tag{2.6g}$$ must be known.

The characteristic equation is obtained by evaluating an $(N+4)$-order determinant.† The result is

$$\left(\frac{D\beta_1}{Dt}\right)^{N+2}\left[\left(\frac{D\beta_1}{Dt}\right)^2 - a^2\left\{\left(\frac{\partial \beta_1}{\partial x}\right)^2 + \left(\frac{\partial \beta_1}{\partial y}\right)^2 + \left(\frac{\partial \beta_1}{\partial z}\right)^2\right\}\right] = 0, \tag{2.7a}$$

where $\beta_1 = \text{const.}$ is a characteristic hypersurface.‡ From this equation it can be seen that there are two sets of real characteristic hypersurfaces given by

$$\frac{D\beta_1}{Dt} = 0, \tag{2.7b}$$

and $$\left(\frac{D\beta_1}{Dt}\right)^2 - a^2\left\{\left(\frac{\partial \beta_1}{\partial x}\right)^2 + \left(\frac{\partial \beta_1}{\partial y}\right)^2 + \left(\frac{\partial \beta_1}{\partial z}\right)^2\right\} = 0. \tag{2.7c}$$

† General characteristic theory is presented by Courant & Hilbert (1962). Those properties and equations of the general theory used in this analysis are summarized in appendix *A* of Sauerwein (1964).

‡ The hypersurface in this case is a three-dimensional manifold in a four-dimensional space.

Equation (2.7*b*) indicates that the particle line is characteristic, and therefore all hypersurfaces made up of particle lines are characteristic. Note that the particle line is an $(N+2)$-fold characteristic because the corresponding term in (2.7*a*) is raised to the $N+2$ power. This means that $N+2$ compatibility equations are available along the particle line. The second characteristic hypersurface given by (2.7*c*) is a quadratic hypersurface which is a generalization of the Mach conoid

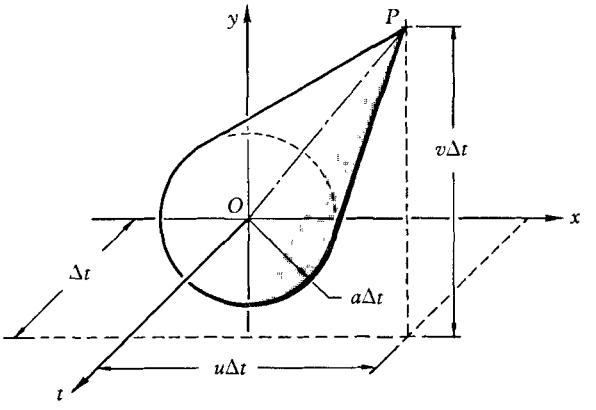

FIGURE 2. Characteristic cone in ordinary fluid dynamics.

that appears in two-dimensional unsteady flow. The general hypersurface can be termed the Mach hyperconoid. The two-dimensional unsteady version of the characteristic hypersurface is shown in figure 2 for the case of a steady, uniform, velocity field. Only the aft-cone in the negative time direction is shown. The cone shown in the figure can be taken as a local approximation to the Mach conoid. In a similar manner, a Mach hypercone can be used as a local approximation to the general Mach hyperconoid and is in the numerical method of characteristics.

For a set of quasi-linear first-order equations of the form

$$\psi_{ijk}\frac{\partial \eta_k}{\partial \alpha_i}+\phi_j=0,$$

a set of linear coefficients λ_j can be found from

$$\lambda_j\psi_{ijk}\frac{\partial \beta_1}{\partial \alpha_i}=0$$

such that at least one compatibility equation for the characteristic surface $\beta_1 = \text{const.}$ can be written in the following form

$$\lambda_j\psi_{ijk}\frac{\partial \beta_2}{\partial \alpha_i}\frac{\partial \eta_k}{\partial \beta_2}+\lambda_j\psi_{ijk}\frac{\partial \beta_3}{\partial \alpha_i}\frac{\partial \eta_k}{\partial \beta_3}+\ldots+G=0.$$

This equation has the useful property that derivatives in a direction normal to the characteristic surface do not appear.

The compatibility equation for the Mach hyperconoid is obtained by determining the λ_i, which have the following form in this case:

$$\lambda_1\rho\frac{\partial\beta_1}{\partial x}+\lambda_2\frac{D\beta_1}{Dt}=0, \tag{2.8a}$$

$$\lambda_1\rho\frac{\partial\beta_1}{\partial y}+\lambda_3\frac{D\beta_1}{Dt}=0, \tag{2.8b}$$

$$\lambda_1\rho\frac{\partial\beta_1}{\partial z}+\lambda_4\frac{D\beta_1}{Dt}=0, \tag{2.8c}$$

$$(\lambda_1+\lambda_2)\frac{D\beta_1}{Dt}=0, \tag{2.8d}$$

$$\frac{1}{\rho}\left(\lambda_2\frac{\partial\beta_1}{\partial x}+\lambda_3\frac{\partial\beta_1}{\partial y}+\lambda_4\frac{\partial\beta_1}{\partial z}\right)-\frac{\lambda_5}{a^2}\frac{D\beta_1}{Dt}=0, \tag{2.8e}$$

$$\left[\lambda_{5+i}+\lambda_5\left\{\left(\frac{\partial h}{\partial c_i}\right)_{p,\rho,c_{j\neq i}}\Big/\left(\frac{\partial h}{\partial\rho}\right)_{p,c_j}\right\}\right]\frac{D\beta_1}{Dt}=0 \quad (i=1,\ldots,N-1). \tag{2.8f}$$

Equations (2.8*a*) to (2.8*d*) and (2.8*f*) can be solved sequentially to give

$$\lambda_2/\lambda_1=-\rho\frac{\partial\beta_1}{\partial x}\Big/\frac{D\beta_1}{Dt}, \tag{2.9a}$$

$$\lambda_3/\lambda_1=-\rho\frac{\partial\beta_1}{\partial y}\Big/\frac{D\beta_1}{Dt}, \tag{2.9b}$$

$$\lambda_4/\lambda_1=-\rho\frac{\partial\beta_1}{\partial z}\Big/\frac{D\beta_1}{Dt}, \tag{2.9c}$$

$$\lambda_5/\lambda_1=-1, \tag{2.9d}$$

$$\lambda_{5+i}/\lambda_1=\left\{\left(\frac{\partial h}{\partial c_i}\right)_{p,\rho,c_{j\neq i}}\Big/\left(\frac{\partial h}{\partial\rho}\right)_{p,c_j}\right\} \quad (i=1,\ldots,N-1). \tag{2.9e}$$

Note that the substitution of these results into (2.8*e*) gives (2.7*c*), which again shows that the correct solution for the homogeneous equations in λ_i has been obtained. These values of λ_i give the compatibility equation which is sought:

$$\begin{aligned}\sum_{m=2}^{4}\Bigg[&\frac{\partial u}{\partial\beta_m}\left\{\frac{\partial\beta_m}{\partial x}\frac{D\beta_1}{Dt}-\frac{\partial\beta_1}{\partial x}\frac{D\beta_m}{Dt}\right\}\\&+\frac{\partial v}{\partial\beta_m}\left\{\frac{\partial\beta_m}{\partial y}\frac{D\beta_1}{Dt}-\frac{\partial\beta_1}{\partial y}\frac{D\beta_m}{Dt}\right\},\\&+\frac{\partial w}{\partial\beta_m}\left\{\frac{\partial\beta_m}{\partial z}\frac{D\beta_1}{Dt}-\frac{\partial\beta_1}{\partial z}\frac{D\beta_m}{Dt}\right\}\\&+\frac{\partial p}{\partial\beta_m}\frac{1}{\rho}\left\{\frac{1}{a^2}\frac{D\beta_m}{Dt}\frac{D\beta_1}{Dt}-\left(\frac{\partial\beta_m}{\partial x}\frac{\partial\beta_1}{\partial x}+\frac{\partial\beta_m}{\partial y}\frac{\partial\beta_1}{\partial y}+\frac{\partial\beta_m}{\partial z}\frac{\partial\beta_1}{\partial z}\right)\right\}\Bigg]\\&+\left[\frac{D\beta_1}{Dt}\Big/\left\{\rho\left(\frac{\partial h}{\partial\rho}\right)_{p,c_i}\right\}\right]\sum_{n=1}^{N-1}\left\{\left(\frac{\partial h}{\partial c_n}\right)_{p,\rho,c_{i\neq n}}r_n\right\}=0.\end{aligned} \tag{2.10}$$

The compatibility equations for the characteristic hypersurfaces made up of particle lines can be determined by inspection to be (2.6*e*) and (2.6*f*) because they contain substantial derivatives only. Using (2.4) instead of (2.6*e*) they are

$$\frac{ds}{d\beta_2} = \frac{-1}{(\partial p/\partial s)_{\rho, c_n}} \sum_{k=1}^{N-1} \left\{ \frac{\partial c_k}{\partial \beta_2} J_k \right\}, \tag{2.11a}$$

where J_k is the quantity in curly brackets in (2.4) and

$$\frac{dc_i}{d\beta_2} = \frac{1}{\rho} r_i \quad (i = 1, \ldots, N-1). \tag{2.11b}$$

The two additional compatibility equations for the particle lines which complete the set of $(N+2)$ equations are the two components of the vector momentum equations projected on the characteristic hypersurface as was shown by von Mises (1958). There are only two components because the vector momentum equation lies completely within the three-space (x, y, z). These last two compatibility equations are not needed for the numerical method of characteristics and are not written here.

Magnetofluid dynamics

The most general case considers the three-dimensional, unsteady flow of a compressible, reacting, multi-component, perfectly conducting fluid where the equations of change have the following form in Cartesian co-ordinates:

$$\frac{D\rho}{Dt} + \rho \left(\frac{\partial u}{\partial x} + \frac{\partial v}{\partial y} + \frac{\partial w}{\partial z} \right) = 0, \tag{2.12a}$$

$$\frac{Du}{Dt} + \frac{1}{\rho}\frac{\partial p}{\partial x} - \frac{1}{\rho\mu}\left\{ B_z \left(\frac{\partial B_x}{\partial z} - \frac{\partial B_z}{\partial x} \right) - B_y \left(\frac{\partial B_y}{\partial x} - \frac{\partial B_x}{\partial y} \right) \right\} = 0, \tag{2.12b}$$

$$\frac{Dv}{Dt} + \frac{1}{\rho}\frac{\partial p}{\partial y} - \frac{1}{\rho\mu}\left\{ B_x \left(\frac{\partial B_y}{\partial x} - \frac{\partial B_x}{\partial y} \right) - B_z \left(\frac{\partial B_z}{\partial y} - \frac{\partial B_y}{\partial z} \right) \right\} = 0, \tag{2.12c}$$

$$\frac{Dw}{Dt} + \frac{1}{\rho}\frac{\partial p}{\partial z} - \frac{1}{\rho\mu}\left\{ B_y \left(\frac{\partial B_z}{\partial y} - \frac{\partial B_y}{\partial z} \right) - B_x \left(\frac{\partial B_x}{\partial z} - \frac{\partial B_z}{\partial x} \right) \right\} = 0, \tag{2.12d}$$

$$\frac{D\rho}{Dt} - \frac{1}{a^2}\frac{Dp}{Dt} + \frac{1}{(\partial h/\partial \rho)_{p, c_n}} \sum_{k=1}^{N} \left\{ \frac{Dc_k}{Dt} \left(\frac{\partial h}{\partial c_k} \right)_{p, \rho, c_{n \neq k}} \right\} = 0, \tag{2.12e}$$

$$\frac{\partial B_x}{\partial t} - \frac{\partial}{\partial y}(uB_y - vB_x) + \frac{\partial}{\partial z}(wB_x - uB_z) = 0, \tag{2.12f}$$

$$\frac{\partial B_y}{\partial t} - \frac{\partial}{\partial z}(vB_z - wB_y) + \frac{\partial}{\partial x}(uB_y - vB_x) = 0, \tag{2.12g}$$

$$\frac{\partial B_z}{\partial t} - \frac{\partial}{\partial x}(wB_x - uB_z) + \frac{\partial}{\partial y}(vB_z - wB_y) = 0, \tag{2.12h}$$

$$\frac{Dc_i}{Dt} = \frac{1}{\rho} r_i \quad (i = 1, \ldots, N-1). \tag{2.12i}$$

Again it will be useful to use (2.4) instead of (2.12*e*) at certain steps below.

The characteristic equation in this case contains an $(N+7)$-order determinant. The expansion of the determinant requires a large amount of algebraic manipulation, but finally gives the following result:

$$\frac{\partial \beta_1}{\partial t}\left(\frac{D\beta_1}{Dt}\right)^N\left\{\left(\frac{D\beta_1}{Dt}\right)^2-(\mathbf{b}.\nabla\beta_1)^2\right\}\left\{\left(\frac{D\beta_1}{Dt}\right)^2-c_f^2\right\}\left\{\left(\frac{D\beta_1}{Dt}\right)^2-c_s^2\right\}=0, \quad (2.13)$$

where $\mathbf{b}$ is the vector Alfvén wave speed

$$\mathbf{b}=\mathbf{B}/\sqrt{(\rho\mu)}, \quad (2.14a)$$

$$b^2=(B_x^2+B_y^2+B_z^2)/\rho\mu, \quad (2.14b)$$

and c_f and c_s are respectively the fast and slow magneto-acoustic wave speeds:

$$c_f^2=\tfrac{1}{2}|\nabla\beta_1|[|\nabla\beta_1|(b^2+a^2)+\{(\nabla\beta_1)^2(b^2+a^2)^2-4a^2(\mathbf{b}.\nabla\beta_1)^2\}^{\frac{1}{2}}], \quad (2.15a)$$

$$c_s^2=\tfrac{1}{2}|\nabla\beta_1|[|\nabla\beta_1|/(b^2+a^2)-\{(\nabla\beta_1)^2(b^2+a^2)^2-4a^2(\mathbf{b}.\nabla\beta_1)^2\}^{\frac{1}{2}}]. \quad (2.15b)$$

Equations (2.12) allow a solution where $\nabla.\mathbf{B}$ is not zero. When $\nabla.\mathbf{B}=0$ is imposed on the set, the $\partial\beta_1/\partial t=0$ root is lost (see Grad 1960). The following characteristic hypersurfaces are obtained in the magnetofluid dynamic case:

$$\frac{D\beta_1}{Dt}=0, \quad (2.16a)$$

$$\left(\frac{D\beta_1}{Dt}\right)^2-(\mathbf{b}.\nabla\beta_1)^2=0, \quad (2.16b)$$

$$\left(\frac{D\beta_1}{Dt}\right)^2-c_f^2=0, \quad (2.16c)$$

$$\left(\frac{D\beta_1}{Dt}\right)^2-c_s^2=0. \quad (2.16d)$$

Equation (2.16*a*) indicates that the particle line is again characteristic, and it can be seen from (2.13) that it is an (N)-fold characteristic. From the similarity of (2.16*b*) to (2.16*d*) with (2.7*c*) it can be seen that these hypersurfaces correspond to three possible waves. These waves are anisotropic, however, having a wave speed which varies with the direction of propagation. They have been studied and their properties examined by Friedrichs & Kranzer (1958). These properties will merely be stated here in order to develop the numerical method. A more complete discussion is given by Jeffrey & Taniuti (1964).

Equation (2.16*b*) corresponds to a transverse wave, termed the Alfvén wave. The other two waves from (2.16*c*) and (2.16*d*) are fast and slow magneto-acoustic waves. These are waves which are partially longitudinal and partially transverse. The wave speed for these three waves can be plotted on a polar plot called a Friedrichs diagram. Such diagrams for the three cases $a^2/b^2>1$, <1, $=1$ are presented in figure 3. The distance from the centre of the plot to a particular point on a curve is the speed of propagation of a wave whose normal vector points in the direction considered. Note that these diagrams are drawn relative to the magnetic induction $\mathbf{B}$, which is taken to be horizontal in the figures. These diagrams have rotational symmetry about $\mathbf{B}$. The inner curve gives the slow magneto-acoustic wave speed, the middle curve gives the transverse wave speed, and the outer curve the fast magneto-acoustic wave speed.

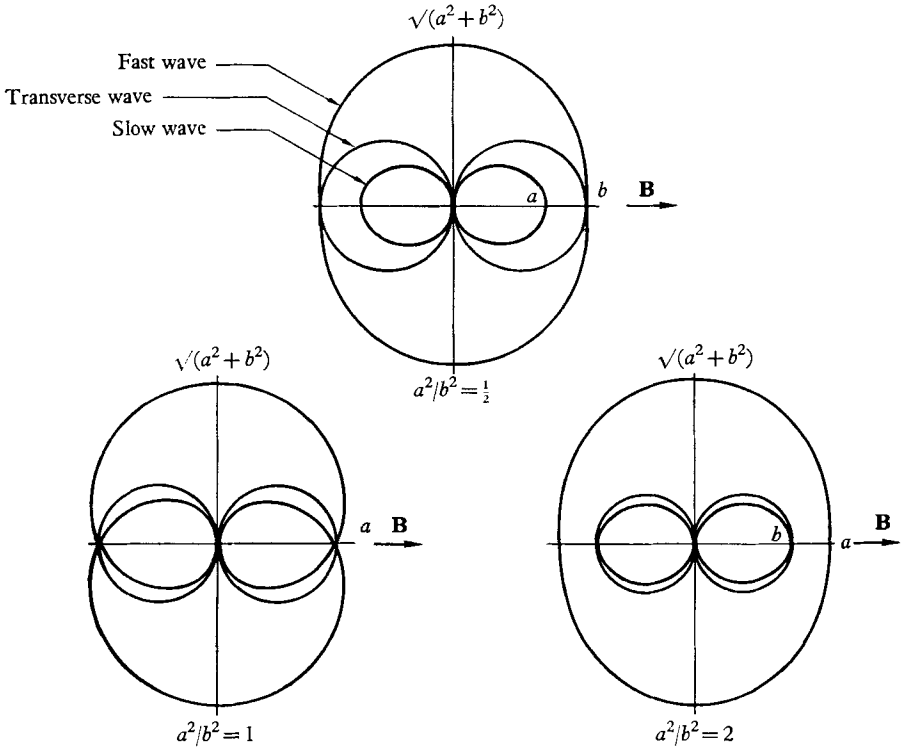

FIGURE 3. Friedrichs diagrams.

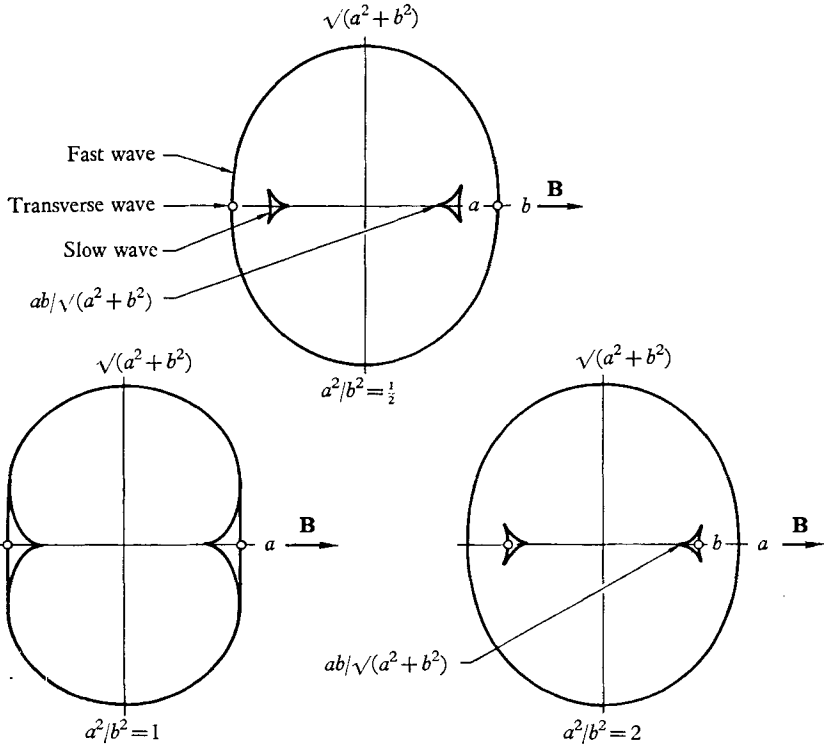

FIGURE 4. Characteristic loci.

The characteristic loci can be obtained from the Friedrichs diagrams by graphical construction or they can be determined analytically. They are shown in figure 4. These loci are the shape of a disturbance that propagates from a point disturbance at the origin in a still medium. It is a picture of the self-similar pulse at a finite time after leaving a point disturbance. Note that the entire disturbed region is within the fast-wave front, but the slow wave is felt throughout the entire

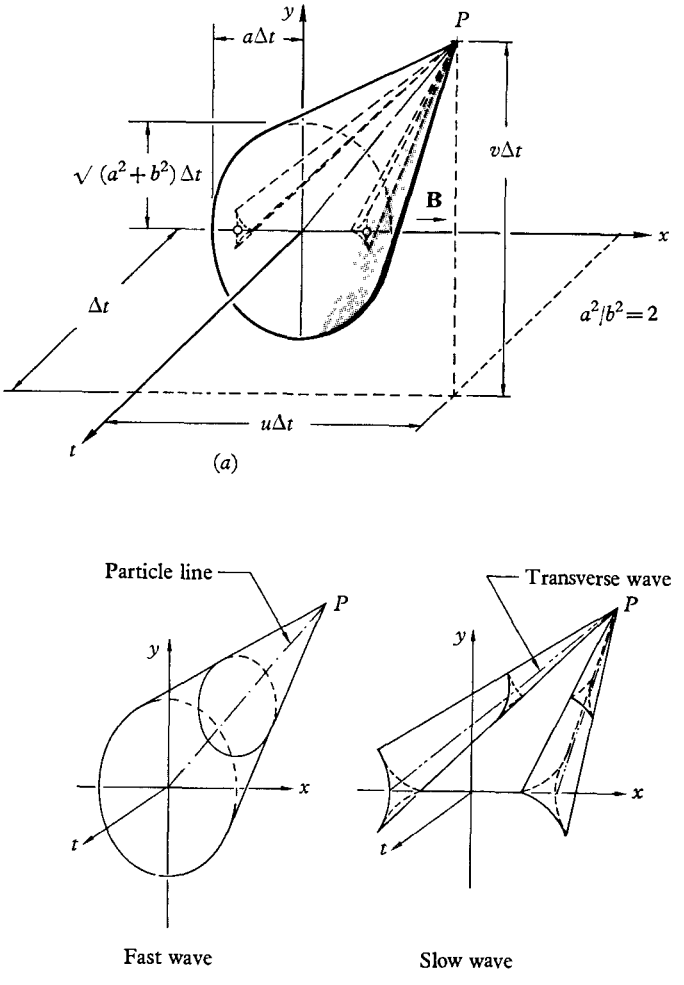

FIGURE 5. Characteristic cones in magnetofluid dynamics. (*a*) Combined and (*b*) separated for clarity.

disturbed region. The two 'cusped triangles' do not bound a region which contains the entire slow-wave disturbance. Sears (1960) has suggested these might be called 'crests,' i.e. discontinuities in the disturbance pattern. The transverse-wave loci become two points indicated by the small circles in figure 4. The characteristic loci also have rotational symmetry about **B**.

Some idea of the geometry of these characteristic hypersurfaces can be obtained by considering the special case of two-dimensional, unsteady flow with

a steady uniform velocity field as was depicted in figure 2 for ordinary fluid dynamics. Figure 5 shows the characteristic surfaces for this case where **B** has been taken parallel to the x-axis. Of the four characteristic surfaces, only the fast and slow waves give true surfaces. The transverse wave surface degenerates into two lines and the particle line, of course, one line. As in the ordinary fluid dynamic case, the characteristic cones (or hypercones in (x, y, z, t)) will be taken in the numerical method as local approximations to the conoids (or hyperconoids).

The compatibility equations are obtained as before, by first solving for the λ_i. First note that the fast- and slow-wave terms in (2.13) really arise from a single fourth-order expression:

$$\left\{\left(\frac{D\beta_1}{Dt}\right)^2 - c_f^2\right\}\left\{\left(\frac{D\beta_1}{Dt}\right)^2 - c_s^2\right\} = \left\{\left(\frac{D\beta_1}{Dt}\right)^4 - (\nabla\beta_1)^2(b^2+a^2)\left(\frac{D\beta_1}{Dt}\right)^2 + (\nabla\beta_1)^2 a^2(\mathbf{b}.\nabla\beta_1)^2\right\} = 0. \quad (2.17)$$

They are both waves which result from an interaction of acoustic and Alfvén waves, as can be seen by the interchange of the roles of a and b in the Friedrichs diagrams when a^2/b^2 is > 1 or < 1. From these properties it can be seen that a single compatibility equation will result for the two waves. The λ_i for the magneto-acoustic waves are given by the following equations:

$$\lambda_1\rho\frac{\partial\beta_1}{\partial x} + \lambda_2\frac{D\beta_1}{Dt} - \lambda_6\left(B_y\frac{\partial\beta_1}{\partial y} + B_z\frac{\partial\beta_1}{\partial z}\right) + \lambda_7 B_y\frac{\partial\beta_1}{\partial x} + \lambda_8 B_z\frac{\partial\beta_1}{\partial x} = 0, \quad (2.18a)$$

$$\lambda_1\rho\frac{\partial\beta_1}{\partial y} + \lambda_3\frac{D\beta_1}{Dt} - \lambda_7\left(B_z\frac{\partial\beta_1}{\partial z} + B_x\frac{\partial\beta_1}{\partial x}\right) + \lambda_8 B_z\frac{\partial\beta_1}{\partial y} + \lambda_6 B_x\frac{\partial\beta_1}{\partial y} = 0, \quad (2.18b)$$

$$\lambda_1\rho\frac{\partial\beta_1}{\partial z} + \lambda_4\frac{D\beta_1}{Dt} - \lambda_8\left(B_x\frac{\partial\beta_1}{\partial x} + B_y\frac{\partial\beta_1}{\partial y}\right) + \lambda_6 B_x\frac{\partial\beta_1}{\partial z} + \lambda_7 B_y\frac{\partial\beta_1}{\partial z} = 0, \quad (2.18c)$$

$$(\lambda_1+\lambda_5)\frac{D\beta_1}{Dt} = 0, \quad (2.18d)$$

$$\frac{1}{\rho}\left(\lambda_2\frac{\partial\beta_1}{\partial x} + \lambda_3\frac{\partial\beta_1}{\partial y} + \lambda_4\frac{\partial\beta_1}{\partial z}\right) - \frac{\lambda_5}{a^2}\frac{D\beta_1}{Dt} = 0, \quad (2.18e)$$

$$-\lambda_2\frac{1}{\rho\mu}\left(B_z\frac{\partial\beta_1}{\partial z} + B_y\frac{\partial\beta_1}{\partial y}\right) + \left(\lambda_3\frac{\partial\beta_1}{\partial y} + \lambda_4\frac{\partial\beta_1}{\partial z}\right)\frac{B_x}{\rho\mu} + \lambda_5\left(\frac{\partial\beta_1}{\partial t} + v\frac{\partial\beta_1}{\partial y} + w\frac{\partial\beta_1}{\partial z}\right) - \lambda_7 v\frac{\partial\beta_1}{\partial x} - \lambda_8 w\frac{\partial\beta_1}{\partial x} = 0, \quad (2.18f)$$

$$-\lambda_3\frac{1}{\rho\mu}\left(B_x\frac{\partial\beta_1}{\partial x} + B_z\frac{\partial\beta_1}{\partial z}\right) + \left(\lambda_4\frac{\partial\beta_1}{\partial z} + \lambda_2\frac{\partial\beta_1}{\partial x}\right)\frac{B_y}{\rho\mu} + \lambda_7\left(\frac{\partial\beta_1}{\partial t} + w\frac{\partial\beta_1}{\partial z} + u\frac{\partial\beta_1}{\partial x}\right) - \lambda_8 w\frac{\partial\beta_1}{\partial y} - \lambda_6 u\frac{\partial\beta_1}{\partial y} = 0, \quad (2.18g)$$

$$-\lambda_4\frac{1}{\rho\mu}\left(B_y\frac{\partial\beta_1}{\partial y} + B_x\frac{\partial\beta_1}{\partial x}\right) + \left(\lambda_2\frac{\partial\beta_1}{\partial x} + \lambda_3\frac{\partial\beta_1}{\partial y}\right)\frac{B_z}{\rho\mu} + \lambda_8\left(\frac{\partial\beta_1}{\partial t} + u\frac{\partial\beta_1}{\partial x} + v\frac{\partial\beta_1}{\partial y}\right) - \lambda_6 u\frac{\partial\beta_1}{\partial z} - \lambda_7 v\frac{\partial\beta_1}{\partial z} = 0, \quad (2.18h)$$

$$\left[\lambda_{8+n} + \lambda_5\left\{\left(\frac{\partial h}{\partial c_n}\right)_{p,\rho,c_{j+n}} \Big/ \left(\frac{\partial h}{\partial\rho}\right)_{p,c_j}\right\}\right]\frac{D\beta_1}{Dt} = 0 \quad (n = 1, \ldots, N-1). \quad (2.18i)$$

Divide (2.18) by λ_1, and solve (2.18*d*) and (2.18*i*) to obtain

$$\lambda_5/\lambda_1 = -1, \tag{2.19a}$$

and

$$\lambda_{8+n}/\lambda_1 = \left(\frac{\partial h}{\partial c_n}\right)_{p,\rho,c_{j\neq n}} \Big/ \left(\frac{\partial h}{\partial \rho}\right)_{p,c_j} \quad (n = 1, \ldots, N-1). \tag{2.19b}$$

Then the remaining λ_i are obtained from the following set of equations obtained from (2.18*a*) to (2.18*c*) and (2.18*f*) to (2.18*h*):

$$\begin{vmatrix}
\frac{D\beta_1}{Dt} & 0 & 0 & -\left(B_y\frac{\partial\beta_1}{\partial y}+B_z\frac{\partial\beta_1}{\partial z}\right) \\
0 & \frac{D\beta_1}{Dt} & 0 & B_x\frac{\partial\beta_1}{\partial y} \\
0 & 0 & \frac{D\beta_1}{Dt} & B_x\frac{\partial\beta_1}{\partial x} \\
-\left(B_z\frac{\partial\beta_1}{\partial z}+B_y\frac{\partial\beta_1}{\partial y}\right) & B_x\frac{\partial\beta_1}{\partial y} & B_x\frac{\partial\beta_1}{\partial z} & \rho\mu\left(\frac{\partial\beta_1}{\partial t}+v\frac{\partial\beta_1}{\partial y}+w\frac{\partial\beta_1}{\partial z}\right) \\
B_y\frac{\partial\beta_1}{\partial x} & -\left(B_z\frac{\partial\beta_1}{\partial z}+B_x\frac{\partial\beta_1}{\partial x}\right) & B_y\frac{\partial\beta_1}{\partial z} & -\rho\mu u\frac{\partial\beta_1}{\partial y} \\
B_z\frac{\partial\beta_1}{\partial x} & B_z\frac{\partial\beta_1}{\partial y} & -\left(B_x\frac{\partial\beta_1}{\partial x}+B_y\frac{\partial\beta_1}{\partial y}\right) & -\rho\mu u\frac{\partial\beta_1}{\partial z}
\end{vmatrix}$$

$$\begin{vmatrix}
B_y\frac{\partial\beta_1}{\partial x} & B_z\frac{\partial\beta_1}{\partial x} \\
-\left(B_z\frac{\partial\beta_1}{\partial z}+B_x\frac{\partial\beta_1}{\partial x}\right) & B_z\frac{\partial\beta_1}{\partial y} \\
B_y\frac{\partial\beta_1}{\partial z} & -\left(B_x\frac{\partial\beta_1}{\partial x}+B_y\frac{\partial\beta_1}{\partial y}\right) \\
-\rho\mu v\frac{\partial\beta_1}{\partial x} & -\rho\mu w\frac{\partial\beta_1}{\partial x} \\
\rho\mu\left(\frac{\partial\beta_1}{\partial t}+w\frac{\partial\beta_1}{\partial z}+u\frac{\partial\beta_1}{\partial x}\right) & -\rho\mu w\frac{\partial\beta_1}{\partial y} \\
-\rho\mu v\frac{\partial\beta_1}{\partial z} & \rho\mu\left(\frac{\partial\beta_1}{\partial t}+u\frac{\partial\beta_1}{\partial x}+v\frac{\partial\beta_1}{\partial y}\right)
\end{vmatrix}
\begin{vmatrix} \frac{\lambda_2}{\lambda_1} \\ \frac{\lambda_3}{\lambda_1} \\ \frac{\lambda_4}{\lambda_1} \\ \frac{\lambda_6}{\lambda_1} \\ \frac{\lambda_7}{\lambda_1} \\ \frac{\lambda_8}{\lambda_1} \end{vmatrix}
= \begin{vmatrix} \rho\frac{\partial\beta_1}{\partial x} \\ \rho\frac{\partial\beta_1}{\partial y} \\ \rho\frac{\partial\beta_1}{\partial z} \\ 0 \\ 0 \\ 0 \end{vmatrix}. \tag{2.19c}$$

The algebraic solution of (2.19*c*) involves an excessive amount of algebraic manipulation. An attempt to invert the matrix in (2.19*c*) by partitioning, in order to take advantage of its symmetry properties, still involves excessive algebraic labour. This indicates that the explicit algebraic solution of (2.19*c*) is very complicated and, therefore, the compatibility equations are also complicated. The ultimate purpose here in obtaining the compatibility equations is to apply them to a numerical method, so it is no drawback to solve (2.19*c*) numerically in order to obtain the compatibility equation with numerical coefficients. The numerical inversion of an 8×8 matrix is a routine procedure for the computer; therefore, in principle, the compatibility equation for the magneto-acoustic waves is determined by the λ_i from (2.19*c*).

Note that equation (2.18*e*) was not used in determining the λ_i. With the substitution of the solution of (2.19*c*) into (2.18*e*), it can be reduced to (2.17). This

is true due to the fact that a solution to the homogeneous set (2.18) is known to exist because of the characteristic equation. The characteristic equation is just the condition required so that a solution to (2.18) exists. If this same procedure were used to obtain the compatibility equation for the transverse Alfvén wave, (2.18*e*) could not be reduced to (2.16*b*) because the former contains the speed of sound a, which cannot be eliminated by substitution of the λ_i from (2.19*c*) because (2.19*c*) does not contain a. Therefore, for the transverse-wave compatibility equation, λ_5 should be set equal to zero, and then, from (2.18*d*) and (2.18*i*) λ_1 and λ_{8+n} are zero. The remaining λ_i are determined from a set of five equations similar to (2.19*c*) where the last equation is omitted, the last column of the square matrix replaces the right-hand side of the equation, and the denominator in the λ_i ratios is λ_8 rather than λ_1. It also appears that this equation must be solved numerically for the same reasons given above for (2.19*c*).

The compatibility equations for the particle line (2.11*a*) and (2.11*b*) are the same as those for the particle line in the ordinary-fluid-dynamic case. Note from (2.13) that there are only N compatibility equations for the particle line in magnetofluid dynamics in contrast to the $N + 2$ equations for the non-conducting case. The two components of the momentum equation are no longer compatibility equations.

This completes the set of equations required for the numerical method of characteristics. The actual numerical techniques and procedures for iterative solution are discussed in the next section.

3. The elements of the numerical-calculation procedure

The numerical method of characteristics is used to solve Cauchy problems for a set of quasi-linear, hyperbolic, partial differential equations. Data are given on an initial non-characteristic hypersurface, together with boundary conditions on the flow field, such as solid body surfaces and shock waves. The solution is then obtained on an adjacent hypersurface by numerical solution of the equations written in characteristic form, i.e. the compatibility equations, with the partial derivatives replaced by their finite-difference approximations. The solution on this new hypersurface is then taken as the initial data, and the process repeated to obtain the solution on the next adjacent hypersurface. In this way, the solution is obtained by matching in space or time until the desired solution is obtained or until the complete region of influence specified by the initial data has been determined.

Only the procedures for calculating the flow at a new point in the flow field away from boundaries are presented here. To determine the flow at a point on the boundary, these procedures must be modified slightly in order to satisfy the boundary conditions at the point. These modifications are straightforward after the basic procedure is defined, and the reader is referred to Butler (1960), Fowell (1961) and Sauerwein (1964) for the details.

One-dimensional unsteady flow

Starting with a simple case to reveal the basic procedure before attempting the more general flows, consider a one-dimensional, unsteady flow of a single-com-

ponent non-conducting fluid. The usual finite difference network for the method of characteristics is shown in figure 6 (*a*). Given the flow properties at points 1 and 2, the new point, numbered 3, is located at the intersection of characteristic lines from 1 and 2. The compatibility equation (see von Mises 1958) written in finite-difference form for the two characteristic lines, becomes

$$\rho_1 a_1 \frac{(u_3-u_1)}{\sqrt{\{(x_3-x_1)^2+(t_3-t_1)^2\}}}+\frac{(p_3-p_1)}{\sqrt{\{(x_3-x_1)^2+(t_3-t_1)^2\}}}=0, \tag{3.1a}$$

$$\rho_2 a_2 \frac{(u_3-u_2)}{\sqrt{\{(x_3-x_2)^2+(t_3-t_2)^2\}}}-\frac{(p_3-p_2)}{\sqrt{\{(x_3-x_2)^2+(t_3-t_2)^2\}}}=0. \tag{3.1b}$$

The denominators, of course, could be eliminated, but they are retained here because, in the more general case to follow, they do not cancel. Simultaneous solution of (3.1) yields u_3 and p_3. From point 3, the particle line is then projected

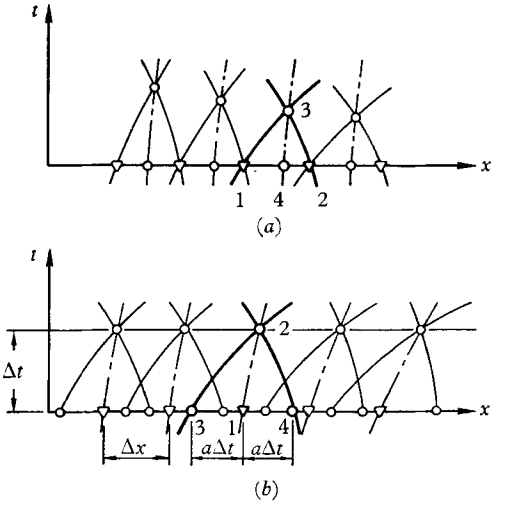

FIGURE 6. One-dimensional networks. ○, Determined points; ▽, initial-data points.

rearward, using the u_3 just determined, to locate the point 4 on the initial line ($t = 0$ in figure 6 (*a*)). From the compatibility equation for the particle line, it is seen that the entropy is constant along the particle line so that

$$s_3 = s_4. \tag{3.2}$$

s_4 must be determined by interpolation among the initial-data points on $t = 0$. This completes the determination of the flow properties at a new point 3. The complete flow field can be built up by repeated application of this basic procedure.

The network proposed here is a slightly modified version of the standard approach. This network was first proposed by Hartree (1953) and is depicted in figure 6 (*b*). The network is constructed by locating the new point 2 a specified constant 'distance' Δt out along the particle line through the initial point 1. Δt can be obtained from

$$\Delta t = \Delta x/2a_{\text{ave}}, \tag{3.3}$$

where a_{ave} is an average speed of sound along the initial-data line and Δx is the initial-data-point spacing. Next, the characteristic lines through 2 are projected

rearward to locate their intersections with the initial-data line at 3 and 4. These points are located a distance $a\Delta t$ on either side of 1. The flow properties at 3 and 4 must be obtained by interpolation. Then the compatibility equations of the form (3.1) determine u_2 and p_2 in terms of the properties at 3 and 4. s_2 is equal to s_1 so that the flow at the new point is determined.

Both of the above procedures can be iterated to second order in the step size by using a modified Euler method. This merely involves repeating the solution of the compatibility equations (3.1) using average values for the coefficient. Thus, for example, in the first network, an equation of the form

$$\tfrac{1}{2}(\rho_1 a_1 + \rho_3^{(n)} a_3^{(n)})\,(u_3^{(n+1)} - u_1) + (p_3^{(n+1)} - p_1) = 0 \tag{3.4}$$

would be iterated in place of (3.1 *a*). The superscript (n) indicates the value of a quantity at the nth-iteration step. This sort of iteration is usually used in most practical calculations.

Hartree's network is proposed here because it would be difficult if not impossible to determine analytically the intersection point corresponding to 3 in figure 6 (*a*) in the case of multi-dimensional, magnetofluid-dynamic flows. On the other hand it is rather simple to determine the intersections with the initial hyperplane of the approximated characteristic hypersurfaces emanating from a point. These intersections are shown in figure 4. Hartree's network has the disadvantage that more interpolation is required, which can introduce more numerical inaccuracies, but it has a secondary advantage for multi-component media in that no interpolation is required on the particle line, and, therefore, more accuracy can be maintained in the usually difficult integration of the rate equation along the particle line. It also has the advantage that the solution is obtained on t = const. lines (or hyperplanes in the general case).

Ordinary fluid dynamics

In generalizing from one-dimensional, unsteady, to three-dimensional, unsteady flow, two fundamental differences occur. One difference is the fact that characteristic *hypersurfaces* arise in the three-dimensional flow while only characteristic *lines* appear in the one-dimensional case. This introduces a 'degree of freedom' in the choice of the network to be used in the multi-dimensional case. This freedom of choice of the net has led to the investigation of various networks and, indeed, Fowell (1961) discussed five different networks proposed by various authors. The main point about the introduction of freedom of choice of the network is that some restrictions must be placed on this freedom in order to ensure numerical stability. This point is discussed in detail below.

The second difference is that the compatibility equations are partial differential equations in the multi-dimensional problem rather than ordinary differential equations as in the one-dimensional case. Hence, derivatives in the β_3 and β_4 directions must be evaluated numerically before the compatibility equations (2.10) can be integrated in the β_2 direction. These derivatives can be evaluated with any one of a number of numerical procedures. A scheme due to Fowell

(1961) is outlined here. For example, consider the u-component of velocity whose partial derivatives can be obtained from the following equations:

$$\frac{\partial u}{\partial \beta_m} = \frac{\partial u}{\partial x}\frac{\partial x}{\partial \beta_m} + \frac{\partial u}{\partial y}\frac{\partial y}{\partial \beta_m} + \frac{\partial u}{\partial z}\frac{\partial z}{\partial \beta_m} + \frac{\partial u}{\partial t}\frac{\partial t}{\partial \beta_m} \quad (m = 3, 4). \tag{3.5a}$$

The $\partial x/\partial \beta_m$, $\partial y/\partial \beta_m$, ... are obtained from the co-ordinate transformation, and the other partial derivatives from

$$(u_5 - u_i) = \frac{\partial u}{\partial x}(x_5 - x_i) + \frac{\partial u}{\partial y}(y_5 - y_i) + \frac{\partial u}{\partial z}(z_5 - z_i) + \frac{\partial u}{\partial t}(t_5 - t_i) \quad (i = 1, \ldots, 4), \tag{3.5b}$$

where the i subscript refers to an initial-data point on the initial hypersurface, and the 5 to the new point being determined. At the first step in the iteration, u_5 can be approximated as

$$u_5^{(0)} = \tfrac{1}{4}(u_1 + u_2 + u_3 + u_4), \tag{3.5c}$$

and, in subsequent steps, a value from the previous iteration is used. The procedure is analogous for the other independent variables.

The co-ordinate transformation

$$\begin{vmatrix} \beta_1 \\ \beta_2 \\ \beta_3 \\ \beta_4 \end{vmatrix} = \begin{vmatrix} \frac{\partial \beta_1}{\partial x} & \frac{\partial \beta_1}{\partial y} & \frac{\partial \beta_1}{\partial z} & \frac{\partial \beta_1}{\partial t} \\ \frac{\partial \beta_2}{\partial x} & \frac{\partial \beta_2}{\partial y} & \frac{\partial \beta_2}{\partial z} & \frac{\partial \beta_2}{\partial t} \\ \frac{\partial \beta_3}{\partial x} & \frac{\partial \beta_3}{\partial y} & \frac{\partial \beta_3}{\partial z} & \frac{\partial \beta_3}{\partial t} \\ \frac{\partial \beta_4}{\partial x} & \frac{\partial \beta_4}{\partial y} & \frac{\partial \beta_4}{\partial z} & \frac{\partial \beta_4}{\partial t} \end{vmatrix} \begin{vmatrix} x \\ y \\ z \\ t \end{vmatrix} \tag{3.6}$$

has only two conditions to fulfil. One is that the characteristic equation must be satisfied, and the other that the β_2-axis must lie along the line from an initial-value point to the new point being determined. It has been found advantageous to use an orthogonal transformation (see Sauerwein 1964) so that, when the two conditions given above are applied together with the orthogonality relations, all but two terms in the transformation matrix can be determined. These two terms can be chosen arbitrarily and correspond to two degrees of freedom left in orienting the orthogonal axes.

The complete numerical procedure can best be seen by referring to figure 7 for two-dimensional unsteady flow. The new point 2 is located out along the particle line from 1 at a 'distance' Δt. The characteristic surface from 2 is projected back to obtain its intersection with the initial surface $t = 0$, which is a circle of radius $a_1 \Delta t$ centred on 1. Three points, numbered 3, 4 and 5, equally spaced on the circle are chosen as the determined initial-data points. Their flow properties are determined by interpolation in the initial-data surface. The compatibility equations (2.18) in finite-difference form for the three lines 3–2, 4–2,

and 5–2 can be solved for u_3, v_3, and p_3 (note that w, z, and β_4 are dropped in this two-dimensional case). The finite-difference form is obtained by introducing for the line 3–2

$$\frac{\partial u}{\partial \beta_2} = (u_2 - u_3)/\sqrt{\{(x_2 - x_3)^2 + (y_2 - y_3)^2 + (t_2 - t_3)^2\}}, \tag{3.7}$$

together with similar equations for the v and p derivatives.

The compatibility equations for the particle line (2.11) are used in a similar manner to determine s_2 and c_{i_2}. A note of warning should be inserted here to indicate that the numerical integration of the reaction-rate equations, i.e. species continuity equations, can be difficult, especially near equilibrium conditions. Sedney & Gerber (1963) have also noted that utilizing entropy in non-equilibrium calculations can lead to large computational errors so that it might be advisable in some cases to use another thermodynamic variable, such as temperature, instead of the more customary quantity, entropy. In many problems of interest the c_i vary much faster along the particle line than the other dependent variables vary along the characteristic surface so that a finer integration step size and a more accurate numerical integration scheme are required along the particle line (see Strom 1965). Another difficulty arises due to the singular nature of the solution as equilibrium conditions are approached in the integration along the particle line. However, new numerical techniques have been developed to overcome this problem; for example, see the work of Treanor (1966) or Morretti (1965).

The above procedure can be iterated to second order in the step size just as in the one-dimensional procedure described above.

A necessary condition for numerical stability is that the domain of dependence of the finite-difference scheme must contain the domain of dependence of the partial differential equations as first pointed out by Courant, Friedrichs & Lewy (1928). The applicability of this condition to the method of characteristics, as opposed to the standard finite-difference approaches (i.e. using rectangular nets), was pointed out by Sauerwein & Sussman (1964). As Heie & Leigh (1965) have indicated the stronger von Neumann condition can also be applied by linearizing the equations and performing a finite-difference calculation. However, both conditions rest ultimately on a heuristic approach due to the lack of an exact test for stability of non-linear partial differential equations. The von Neumann condition requires the development and checking of a computer program just to test stability heuristically, while the Courant–Friedrichs–Lewy condition is simply applied to the geometry of the finite-difference network. It would appear that it might be simpler to apply the CFL condition and program the complete calculation, which could be checked heuristically for stability with a known flow field rather than to program a complicated finite-difference procedure only to check for stability.

The CFL condition is applied to the finite-difference network next. In figure 7 this means that the square formed by the outer fixed data points used in the interpolation to determine the flow properties at 3, 4 and 5 must contain the circle through 3, 4 and 5. In general, this means that the figure obtained by connecting with straight lines the outermost, fixed initial-data points used in the

interpolation must contain the figure which is the intersection of the characteristic hypersurface with the initial hypersurface.

The three-dimensional, unsteady case can now be considered. As in the two-dimensional case, the new point is located at a perpendicular distance Δt from the initial hyperplane out along a particle line through a fixed initial point. The rearward, i.e. in the negative time direction, characteristic hypersurface

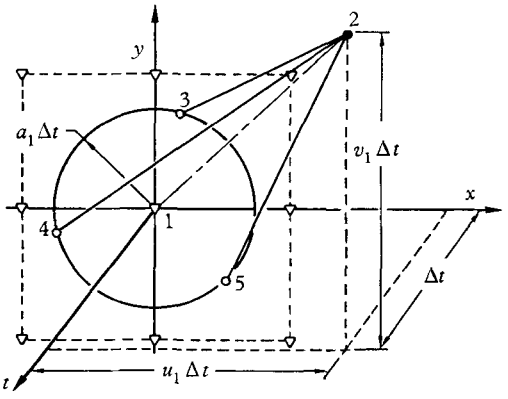

FIGURE 7. Finite-difference network in ordinary fluid dynamics. ▽, Fixed initial-data points in $t = 0$; ○, determined initial points in $t = 0$; ●, new point.

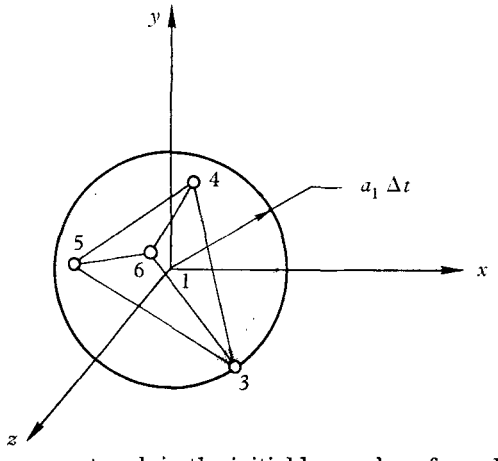

FIGURE 8. Finite-difference network in the initial hyperplane for ordinary fluid dynamics.

is projected back to obtain its intersection with the initial hypersurface. This intersection is approximated as a sphere of radius $a_1 \Delta t$ centred on the fixed initial-data point as shown in figure 8. The compatibility equation (2.10) in finite-difference form must be written for four lines from the initial hyperplane to the new point in order to determine the four unknown quantities u_2, v_2, w_2, and p_2. The four determined initial points, numbered 3 to 6 in figure 8, should be evenly spaced on the sphere and this can be done by locating them at the corners of a regular tetrahedron inscribed within the sphere. s_2 and c_{i_2} are determined as described above for the two-dimensional case, and the iteration scheme is exactly the same. Hence, all the flow properties at a new point in the flow field can be determined.

Magnetofluid dynamics

The magnetofluid-dynamics case can be handled in exactly the same manner as the ordinary-fluid-dynamics finite-difference network. The only difference is in the location of the determined initial points on the intersection of the characteristic hypersurface with the initial hypersurface.

It is simpler to first consider a two-dimensional, unsteady case. The proposed locations of the determined initial-data points are shown in figure 9. Point 1 is the fixed initial-data point at the base of the particle line that determines the location of the new field point. Points 2 and 3 are at the base of the transverse wave lines, while 4 to 9 are on the slow-wave 'crest'; 10 to 13 are on the fast-wave front. The 13 points would seem to be the minimum number necessary in order to account for all disturbances in the domain of dependence while still retaining the symmetries of the figure. The points on the slow-wave intersection have been located on the cusps (points 4 to 9) because these might be the points which carry the dominant part of the slow-wave disturbance. Cumberbatch (1962) has found that this is the case for the points 5 and 7 in steady flow.

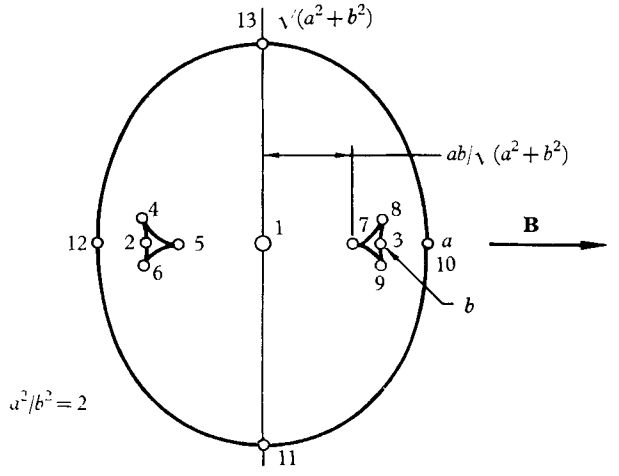

FIGURE 9. Location of determined initial-data points for two-dimensional magnetofluid dynamics.

With s and c_i determined by the compatibility equations along the particle line, twelve other compatibility equations are left to determine the five unknowns u, v, p, B_x, and B_y. These equations can either be solved in a least squares sense, or seven of the fifty partial derivatives in the β_3 direction can be taken as additional unknowns rather than evaluating them numerically. The former would seem to be the better procedure in that the arbitrary choice of the specific seven derivatives to be considered unknown would probably affect the accuracy of the results in some not easily predictable manner.

Finally, the determined initial points for the three-dimensional unsteady case can be located as shown in figure 10. The x-axis has been aligned with the local **B** and the two intersection surfaces have been separated for clarity. Both surfaces have rotational symmetry about **B**. The minimum number of points

appears to be 16. Of course more could be used, but this would just introduce more equations to be solved without increasing the number of unknowns. For the network of figure 10 there are fifteen equations in seven unknowns, u, v, w, p, B_x, B_y, and B_z, neglecting the particle line through 1 which determines s and c_i independently. The solution can be obtained in the same manner as suggested above for the two-dimensional case.

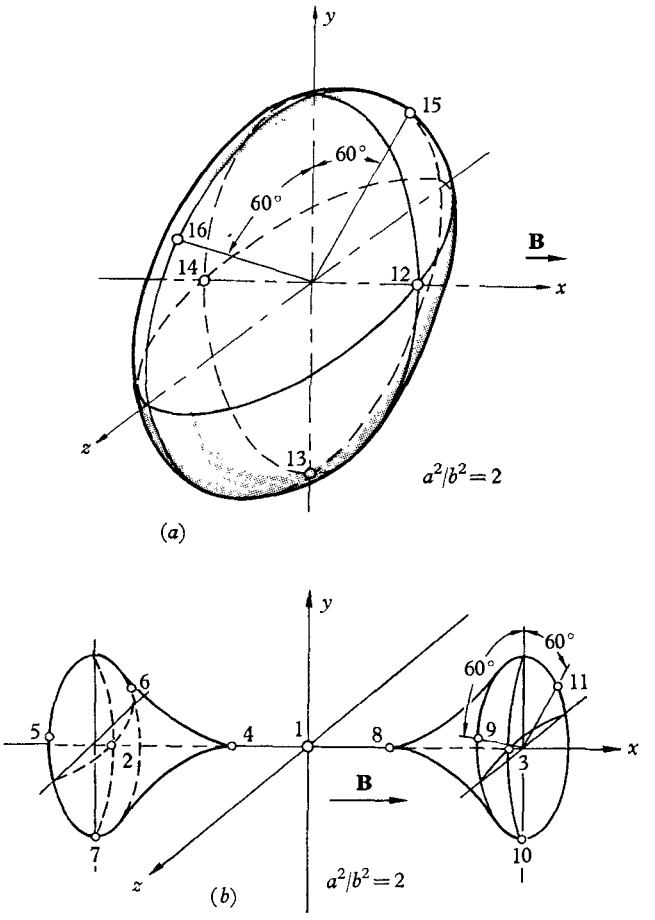

FIGURE 10. Location of determined initial-data points for three-dimensional magnetofluid dynamics. (*a*) The fast-wave surface, and (*b*) the slow-wave surface.

4. Preliminary numerical results

It is not the purpose of this paper to present the results of a tested and developed numerical procedure. The purpose is to present the theory underlying the new procedure and the details of the numerical network together with its inherent advantages, which it is believed vastly outweigh its disadvantages. However, it is in order to indicate the degree of confidence one might place in the method as to obtaining successful results efficiently. With this in mind a sample of preliminary numerical results being obtained with the method is given in this section.

First, it should be noted that the programming of the numerical procedure is not a simple task. Approximately four man-years were required to write the program for the calculation of two-dimensional, unsteady ordinary fluid dynamics of a perfect gas. The program uses linear interpolation throughout. This was done in order to obtain a working program as soon as possible so that the stability and feasibilities of the procedure could be evaluated in the shortest period of time.

A network similar to that shown in figure 6 (*a*) was used because the advantages of the network in figure 6 (*b*) are more favourable for reacting and magnetofluid effects. However, in the process of adding higher-order interpolation to the programs, which is being done at the present time, the network is being switched from the (*a*) type to the (*b*) type. Thus, future additions of chemical reactions or other improvements will be simpler.

In order to develop and test the procedure, the flow between a detached shock wave and the surface of a two-dimensional body in unsteady motion has been calculated. The motion of the body is arbitrary as long as no additional shock waves (other than the bow shock) are introduced into the flow. Initial, steady-state data for the flow of a perfect gas (specific heat ratio equal to 7/5) at a Mach number of 5 over a circular cylinder were obtained from the work of Belotserkovskii (1958). The body surface was warped or oscillated in time to disturb the steady-flow field.

Some of the results of one such calculation appear in figure 11.† The circular cross-section of the cylinder was warped to an ellipse whose semi-major axis was 7 % greater than the radius of the cylinder. The semi-major axis of the ellipse grew in time using one-half period of a cosine function displaced by one-half its amplitude. The semi-major axis was located at a positive angle of attack of 20°. The equations for the motion of the body surface are

$$B(x,y,t) = \frac{4\{x^2\cos^2\alpha - xy\sin 2\alpha + y^2\sin^2\alpha\}}{\{(A-1)\cos[\pi(1+t/t_0)]+A+1\}^2} + x^2\sin^2\alpha + xy\sin 2\alpha + y^2\cos^2\alpha - 1 = 0 \quad \text{for} \quad 0 \leqslant t \leqslant t_0, \tag{4.1a}$$

$$B(x,y,t) = x^2\left(\frac{\cos^2\alpha}{A^2}+\sin^2\alpha\right) + xy\left(1-\frac{1}{A^2}\right)\sin^2\alpha + y^2\left(\frac{\sin^2\alpha}{A^2}+\cos^2\alpha\right) - 1 = 0 \quad \text{for} \quad t > t_0, \tag{4.1b}$$

where for figure 11 $\alpha = 20°$, $A = 1{\cdot}07$, $t_0 = 8\times10^{-5}$ sec. The body motion has stopped by time step 14. Figure 11 shows the velocity-vector field plotted for the time steps indicated. This plot was generated directly by the computer. The computer can also be used to generate contour plots of any of the thermodynamic variables or the Mach number.

Each of these time-step results lies on an almost planar time surface. Linear interpolation was used on the 8th, 16th, 24th and 32nd time steps to give the results on constant-time planes. When the implementation of network (*b*) of

† Results for intervening stages of the calculation are being held in the editorial files and may be obtained from the editor if required.

figure 6 has been completed, this additional interpolation will not be necessary. It can be noted in figure 11 that the net does not maintain a regular spacing and decreases slightly in size even though the calculation is initially carried well into the supersonic region. These effects will also be eliminated with network (*b*).

In the plots of figure 11 the compression wave can be seen developing on the moving body surface and propagating asymmetrically into the flow field. Figure 11 follows the wave to the point where it interacts with the bow shock wave. Beyond this point the wave is difficult to follow in the velocity-vector field because the two-dimensional spreading effect reduces its amplitude. It can be seen in pressure plots, however. The calculation has been carried some 60 time steps, but due to the repeated use of linear interpolation the accuracy decreases to the point that the later time steps are only qualitatively useful. The addition of higher-order interpolation, under way at the present time, should considerably increase the number of time steps that can be accurately calculated.

The calculation was performed on an IBM 7094 II computer. The calculation and plot generating required approximately 90 min of computer time for the 60 time steps. The plot generating was done after the calculation as both the calculation and plotting programs could not be held in the 32,000-word computer memory at the same time. Details of the problems encountered in programming and extensive numerical results will be published later.

5. Conclusions

First, it should be evident from the development in this paper that the numerical method of characteristics can be applied to simpler specialized problems as well as the most general three-dimensional unsteady flow of a perfectly conducting, inviscid, reacting, multi-component fluid. The method can also be applied to steady flows where the local velocity is everywhere greater than the largest local wave speed or, in other words, when the partial differential equations are hyperbolic. Some care must be taken, however, in determining the characteristic surfaces for magnetofluid-dynamic steady flow (see Grad 1960, and Cumberbatch 1962).

The preliminary numerical results indicate that the multi-dimensional method of characteristics presented here can be used to obtain useful results with a reasonable effort. These preliminary results have indicated certain improvements to the method which can increase its utility and efficiency. These improvements have been incorporated in the new finite-difference network presented here and would seem to aid the extension of the method to four-independent-variable problems with chemical reactions and magnetofluid-dynamic effects.

One limiting aspect of the numerical method of characteristics is the large amount of initial data required to start the solution. Many theories are available to give certain specific details of flow fields, but the complete details of entire flow fields are seldom determined and hardly ever published. For this reason, the application of the method might be somewhat limited, but there is the intriguing possibility of specializing the general method in certain cases so that it could determine its own initial data. For example, the initial conditions for a three-dimensional unsteady flow in ordinary fluid dynamics might be obtained

by using a specialized form of the general method to solve a three-dimensional steady supersonic flow.

The solution of unsteady, two-dimensional flow for ordinary fluid dynamics is feasible and practical at the present time utilizing presently available high-speed, electronic digital computers as shown by the work of Butler (1960), Sauerwein (1964) and the new results presented here. The solution of three-dimensional, steady flows in ordinary fluid dynamics has been accomplished by Tsung (1960), Morretti *et al.* (1962) and Strom (1965). Calculating the more difficult problems involving multi-component, non-equilibrium thermodynamics in three-dimensional, unsteady flows with magnetic effects is marginal with existing computers. These calculations should become completely feasible, at least for the simpler cases, with the next generation of computers, which will appear shortly.

It appears that there are vast possibilities for the utilization of high-speed, electronic digital computers, and the numerical method of characteristics in solving complicated non-linear fluid-dynamics problems. This is especially true when very general boundary conditions and complicated physical processes must be considered.

The author wishes to thank Professor Holt Ashley of the Massachusetts Institute of Technology for his inspiration and initial guidance; Professor Adolf Busemann of the University of Colorado, for his comments and criticism, and to acknowledge several stimulating discussions with Professor James T. Yen of the Catholic University of America. The assistance of Mark Sussman and John Szabo with the programming of the numerical procedure is also gratefully acknowledged.

REFERENCES

BELOTSERKOVSKII, O. M. 1958 Flow past a circular cylinder with a detached shockwave. *Vychislitelnaia Mathematika*, **3**, 149.

BROER, L. J. F. 1958 Characteristics of the equations of motion of a reacting gas. *J. Fluid Mech.* **4**, 276.

BRUHN, G. & HAACK, W. 1958 Ein Charakteristikenverfahren für drei-dimensionale instationäre Gasströmungen. *Math. Phys.* **9**, 173.

BUTLER, D. S. 1960 The numerical solution of hyperbolic systems of partial differential equations in three independent variables. *Proc. Roy. Soc.* A, **255**, 232.

CHU, B. T. 1957 Wave propagation and the method of characteristics in reacting gas mixtures with applications to hypersonic flow. *WADC TN*, no. 57-213.

COBURN, N. & DOLPH, C. L. 1949 The method of characteristics in the three-dimensional stationary supersonic flow of a compressible gas. *Proc. Symp. Appl. Math.* **1**, 55.

COURANT, R., FRIEDRICHS, K. O. & LEWY, H. 1928 Über die partiellen Differenzialgleichungen der mathematischen Physik. *Math. Ann.* **100**, 32.

COURANT, R. & HILBERT, D. 1962 *Methods of Mathematical Physics Vol. II, Partial Differential Equations*, chap. VI. New York and London: Interscience.

CUMBERBATCH, E. 1962 Magnetohydrodynamic Mach cones. *J. Aero. Sci.* **29**, 1476.

FERRI, A. 1954 The method of characteristics, section G of *General Theory of High Speed Aerodynamics*, vol. VI of *High Speed Aerodynamics and Jet Propulsion*. Princeton University Press.

FOWELL, L. F. 1961 Flow field analysis for lifting re-entry configurations by the method of characteristics. *I.A.S. Paper*, no. 61-208-1902.

FRIEDRICHS, K. O. & KRANZER, H. 1958 Notes on magneto-hydrodynamics, no. VIII. Nonlinear wave motion. *N.Y.U. Rep* no. NYO-6486-VIII.

GRAD, H. 1960 Reducible problems in magneto-fluid dynamic steady flow. *Rev. Mod. Phys.* **32**, 830.

HARTREE, D. R. 1953 Some practical methods of using characteristics in the calculation of non-steady compressible flow. *U.S. Atomic Energy Comm. Rep* no. AECU-2713.

HEIE, H. & LEIGH, D. C. 1965 Numerical stability of hyperbolic equations in three independent variables. *A.I.A.A. J.* **3**, 1099.

HOLT, M. 1956 The method of characteristics for steady supersonic rotational flow in three dimensions. *J. Fluid Mech.* **1**, 409.

JEFFREY, A. & TANIUTI, T. 1964 *Non-linear Wave Propagation with Applications to Physics and Magnetohydrodynamics*. New York and London: Academic Press.

MEYER, R. E. 1953 The method of characteristics, in *Modern Developments in Fluid Dynamics, High Speed Flow*, pp. 71–104. London: Oxford University Press.

VON MISES, R. 1958 *Mathematical Theory of Compressible Fluid Flow*, pp. 100–15. New York: Academic Press.

MORRETTI, G., SANLORENZO, E. A., MAGNUS, E. E. & WEITERSTEIN, G. 1962 Flow field analysis of reentry configurations by a general three-dimensional method of characteristics. *ASD-TR*-61-272, vol. III.

MORRETTI, G. 1965 A new technique for the numerical analysis of non-equilibrium flows. *A.I.A.A. J.* **3**, 223.

SAUER, R. 1950 Dreidimensionale Probleme der Charakteristikentheorie partieller Differential-Gleichungen. *Z. ang. Math. Mech.* **30**, 347.

SAUERWEIN, H. 1964 The calculation of two- and three-dimensional inviscid unsteady flows by the method of characteristics. M.I.T. Sc.D. thesis; *Fluid Dyn. Lab. Rep* no. 64-4, AFOSR 64-1055.

SAUERWEIN, H. & SUSSMAN, M. 1964 Numerical stability of the three-dimensional method of characteristics. *A.I.A.A. J.* **2**, 387.

SEARS, W. R. 1960 Some remarks about flow past bodies. *Rev. Mod. Phy.* **32**, 701.

SEDNEY, R. & GERBER, N. 1963 Non-equilibrium flow over a cone. *I.A.S. Paper*, no. 63-71.

STROM, C. R. 1965 The method of characteristics for three-dimensional steady and unsteady reacting gas flow. Ph.D. thesis, Univ. of Illinois.

THORNHILL, C. K. 1948 The numerical method of characteristics for hyperbolic problems in three independent variables. *A.R.C. R & M*, no. 2615.

TREANOR, C. E. 1966 A method for the numerical integration of coupled first order differential equations with greatly different time constants. *Maths Comput.* **20**, 39.

TSUNG, C. C. 1960 Study of three-dimensional supersonic flow problems by a numerical method based on the method of characteristics. Ph.D. thesis, Univ. of Illinois.